Available online at www.sciencedirect.com
ScienceDirect
Ore Geology Reviews 34 (2008) 263–270
ORE GEOLOGY REVIEWS
www.elsevier.com/locate/oregeorev

Single grain pyrite Rb–Sr dating of the Linglong gold deposit, eastern China

Qiu-Li Li [a,b], Fukun Chen [a,b,*], Jin-Hui Yang [a], Hong-Rui Fan [a]

[a] Key Laboratory of Mineral Resources, Institute of Geology and Geophysics, Chinese Academy of Sciences, Beijing, 100029, People's Republic of China
[b] Laboratory for Radiogenic Isotope Geochemistry, Institute of Geology and Geophysics, Chinese Academy of Sciences, Beijing, 100029, People's Republic of China

Received 23 October 2006; accepted 9 October 2007
Available online 28 November 2007

Abstract

This study employs the single grain pyrite Rb–Sr technique to date mineralization, using the example of the Linglong lode gold deposit, Jiaodong Peninsula, eastern China. The gold deposits in this area are interpreted to have a consistent spatial–temporal relationship with widespread Late Jurassic–Early Cretaceous magmatism in eastern China, likely related to lithospheric thinning around 120 Ma. Pyrite of the Linglong gold mine contains different types of mineral inclusions such as sericite and feldspar that cause distinguishable variations in Rb- and Sr contents and Rb/Sr ratios. Four pyrite samples from veins of different mineralization stages give an average isochron age of 120.6±0.9 Ma. Analyses of one quartz and two sericite samples yield isochron ages between 122 Ma and 120 Ma. Dating of mineralization is often hampered by disequilibrium of isotopic systems and/or the lack of suitable minerals for dating purposes. Hence, the successful attempt of the single grain Rb–Sr technique of pyrite, which occurs as a common mineral phase in orebodies and is genetically related to the mineralization, has great potential for precise geochronology of hydrothermal mineral deposits.

Keywords: Pyrite; Single grain; Rb–Sr dating; Gold deposit; Mineral inclusion

1. Introduction

Dating of hydrothermal mineral deposits is often difficult to achieve but, nevertheless, critical for understanding the relationship between the timing of mineralization and geological events (e.g., Jiang et al., 2000). Numerous studies have been aimed at the direct dating of mineralization on sulfide minerals, for example, the Rb–Sr dating of sphalerite and pyrite (e.g., Nakai et al., 1990; Brannon et al., 1992; Yang and Zhou, 2001), the Sm–Nd dating of sphalerite, galena and pyrite (e.g., Jiang et al., 2000), and the Re–Os dating of molybdenite and other sulfides (e.g., McCandless et al., 1993; Frei et al., 1998; Lambert et al., 1999; Stein et al., 2000; Barra et al., 2003; Morelli et al., 2004; Trista-Aguilera et al., 2006). Nevertheless, routine application of these methods to constrain mineralization ages is often hampered by various reasons: (1) lack of suitable minerals for geochronological purposes, (2) disequilibrium of isotopic systems of minerals during the formation of ores, and (3) limitations due to high procedural blank and low sensitivity of thermal ionization mass spectrometer (TIMS). Most ore-forming minerals have low parent/daughter ratios and/or low contents of the relevant elements, making reliable age determination difficult (Brannon et al., 1992). Hence, more than 100 mg of sample material (even 1000 mg) are usually used for conventional analysis to overcome the shortcomings of high procedural blanks and low sensitivity of thermal ionization mass spectrometer. The use of large quantities of sample material, however, frequently averages out variations in parent/daughter ratios, resulting in lower precision of the isochron ages.

To place age constraints on gold lode deposits, indirect methods are also often employed, including K–Ar and Rb–Sr dating of alteration minerals such as sericite, or the Rb–Sr dating of fluid inclusions in quartz (e.g., Böhlke and Kistler, 1986; Luo and Wu, 1987; Zhang et al., 1994). Conventional

* Corresponding author. Laboratory for Radiogenic Isotope Geochemistry, Institute of Geology and Geophysics, Chinese Academy of Sciences, Beijing, 100029, People's Republic of China. Fax: +86 10 62010846.
E-mail address: fukun-chen@mail.igcas.ac.cn (F. Chen).

0169-1368/$ - see front matter © 2007 Elsevier B.V. All rights reserved.
doi:10.1016/j.oregeorev.2007.10.003

Rb–Sr dating is generally performed via isochron techniques, mostly with sample suites containing different minerals and/or whole rocks. A prerequisite for a valid isochron relationship between minerals and/or whole rocks is the attainment of initial Sr isotope equilibrium without later alteration (e.g., Zheng, 1989). However, many factors can critically influence the validity of isochrons defined from different minerals and/or whole rocks. Amongst them are petrological processes such as partial melting, fractional crystallization or magma mixing, sequent (or non-coeval) mineral precipitation, subsequent thermal metamorphism, the infiltration of fluids, and, to some extent, deformation. In particular fluids act as catalyzing agents and can enhance reactions and element transport (e.g., Zheng, 1989; Villa, 1998). Thus, the ages obtained by the Rb–Sr isochron method of different minerals and/or whole rocks can vary considerably or are characterized by large errors (e.g., Zhang et al., 1994).

Recent improvements in chemical procedures to lower the blank levels and in mass spectrometric (TIMS) techniques enable precise measurement on micro samples containing less than 1 ng Sr (Chen et al., 1996; Müller et al., 2000a,b; Li et al., 2005; Charlier et al., 2006). A combination of these techniques provides an opportunity to analyze mica, pyrite, quartz, and other minerals within orebodies by the single grain technique for dating purposes. Pyrite, sericite and quartz occurring as common minerals in gold deposits or are genetically related to mineralization in other types of ore deposits. Dating these minerals can provide direct constraints on mineralization ages.

Previous attempts at pyrite dating have been made using the Pb–Pb, Re–Os, Ar–Ar, and Rb–Sr techniques (Freydier et al., 1997; Frei et al., 1999; Smith et al., 2001; Yang and Zhou, 2001; Philips and Miller, 2006). Successful dating using conventional Rb–Sr analysis was achieved on large amounts of acid-leached pyrite collected from the Linglong gold deposit, Shandong Province in eastern China (Yang and Zhou, 2001). Although each sub-sample of pyrite taken for analysis weighed more than 500 mg, $^{87}Rb/^{86}Sr$ ratios of such sub-samples from the same hand specimen were significantly different from each other. Fluid inclusions in pyrite were considered as a major factor causing the variations in Rb/Sr ratios (Yang and Zhou, 2001). In the present study, we re-examined pyrite from the Linglong gold deposit using scanning electron microscopy to investigate mineral inclusions in pyrite. We then employed the single grain (or micro-sample) Rb–Sr dating method to analyze pyrite, quartz and sericite from the mineralized veins. The role of mineral inclusions in the pyrite Rb–Sr dating of mineralization is also discussed.

2. Geological setting and previous geochronological work

The Linglong gold mine is situated in the northwestern part of the Jiaodong Peninsula, eastern Shandong Province (Fig. 1). This area is the largest repository of gold (>35 Moz Au) in China based on historical production rates. Most of the gold deposits are distributed between the Tanlu fault zone and the Wulian–Qingdao–Yantai fault. The latter is considered as the boundary between the North China Craton and the Sulu ultrahigh-pressure (UHP) orogenic belt (e.g., Zhai et al., 2000). The northwestern Jiaodong Peninsula is composed mainly of Precambrian metamorphic sequences, Mesozoic volcanic rocks and granitoids, and minor Mesozoic sedimentary cover rocks (e.g., Li and Yang, 1993; Wang et al., 1998). The Precambrian sequences mainly comprise the Late Archean amphibolite to granulite facies Jiaodong Group and the Proterozoic Fenzishan and Penglai Groups, which are composed of low-grade metasedimentary rocks. The Jiaodong Group, dated at 2665± 9 Ma using the U–Pb zircon method (Qiu, 1989), consists mainly of mafic to felsic volcanic and sedimentary rocks and is interpreted as an Archean greenstone belt (Ji et al., 1994). The Mesozoic granitoids that intrude the high-grade Jiaodong Group can be subdivided into three groups according to compositional and textural characteristics and field relationships (Qiu et al., 2002): (1) a granite–granodiorite group mainly comprising biotite granites, granodiorites and monzonites; (2) a porphyritic granodiorite group consisting of porphyritic, hornblende-bearing granodiorites, monzogranites and granites; (3) a peralkaline granitoid group consisting mainly of monzonites and syenites. Most of the large gold mines in the Jiaodong Peninsula are hosted in the widely-distributed metaluminous to slightly peraluminous granitoids of the first two groups. These include the Linglong and Jiaojia gold deposits hosted in the 160 Ma to 156 Ma old Linglong medium-grained biotite granite and the 130 Ma to 126 Ma old Guojialing porphyritic granodiorite (e.g., Miao et al., 1997; Wang et al., 1998; Guan et al., 1998).

The large gold deposits of the Jiaodong Peninsula are mainly distributed, from west to east, in the Zhaoyuan–Laizhou (or Zhao–Ye), the Qixia–Yantai, and the Rushan–Mouping gold belts (e.g., Wang et al., 1998; Qiu et al., 2002; Fig. 1a). Two types of gold deposits have been identified, i.e., the Linglong type of Au-bearing quartz lode gold and the Jiaojia type of hydrothermal alteration accompanied by disseminated pyrite and gold without the development of quartz veins. The gold deposits in this area have a consistent spatial–temporal association with the Late Jurassic–Early Cretaceous magmatism (ca. 130 Ma to 110 Ma) in eastern China, which is interpreted to be related to lithospheric thinning (e.g., Wang et al., 1998; Yang et al., 2003 and references therein). Detailed information about the geological setting and genesis of gold lode deposits was outlined in previous studies (e.g., Wang et al., 1998; Yang and Zhou, 2001; Qiu et al., 2002; Zhai et al., 2002; Fan et al., 2003, 2005; Li et al., 2003; Yang et al., 2003; Zhang et al., 2003; Chen et al., 2005).

The so-called Linglong-type quartz vein-style gold deposits are typically hosted in second- or third-order faults cutting the Mesozoic Linglong granitoids. The gold mineralization occurs as single or multiple, relatively continuous quartz veins, which can be as long as 5 km. The veins range from a few cm to a few meters in width, and extend down dip for at least a few hundred meters. More than 50 auriferous quartz veins occur within the Linglong area (Fig. 1b). The quartz veins are translucent to milky and gray in color, and sometimes zoned from a central massive sulfide zone as thick as 1 m. They consist of pyrite and minor chalcopyrite, galena, and sphalerite, to marginal zones quartz–pyrite assemblages. They appear to fill pre-existing faults, as they are commonly bounded by fault gouges or thin zones with quartz and sericite. The veins may contain fragments of country rock and rarely cut the foliation of the fault gouge,

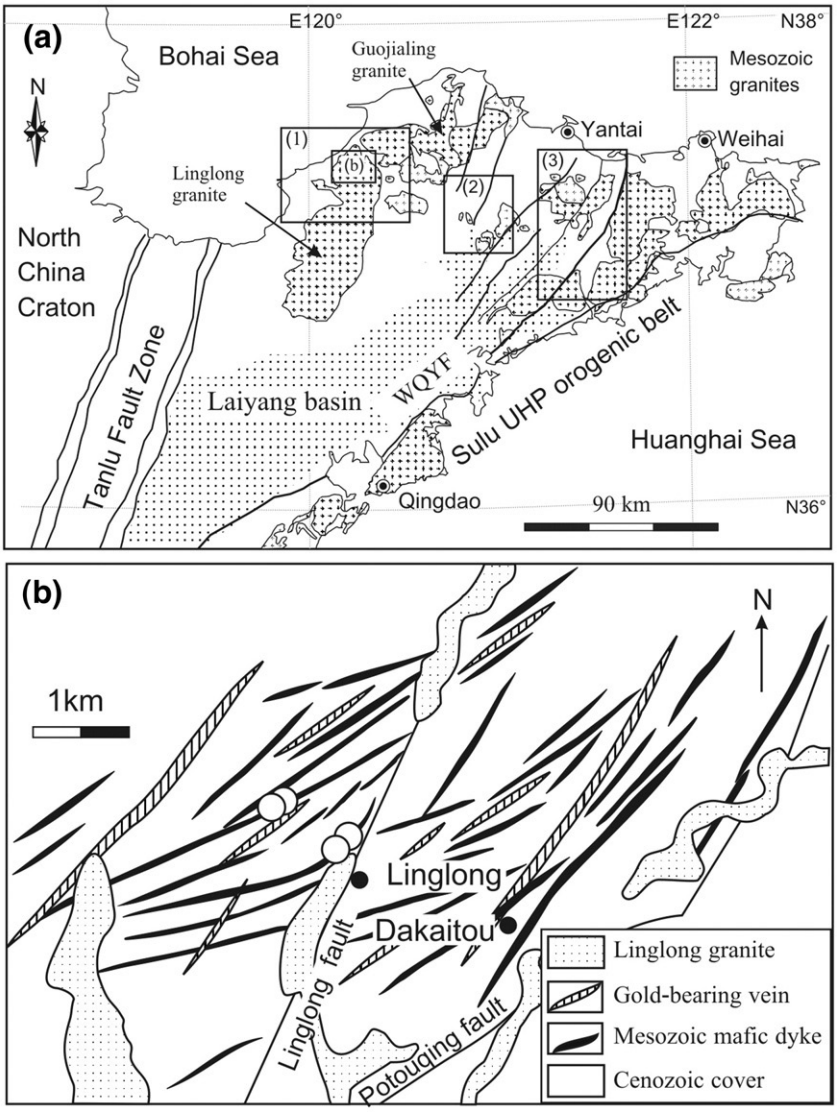

Fig. 1. (a) Simplified geological map of the Jiaodong Peninsula, eastern China. Three gold mineralization zones in the peninsula are identified after e.g., Wang et al. (1998) and Qiu et al. (2002): (1) the Zhaoyuan–Laizhou (Zhao–Ye) gold belt; (2) the Qixia–Yantai gold belt; (3) the Rushan–Mouping gold belt. WQYF: Wulian–Qingdao–Yantai fault. (b) Study area of the Linglong gold mine (after Yang and Zhou, 2001).

suggesting that at least some of the hosting faults were formed prior to the quartz veins. Wallrock alteration adjacent to the quartz veins commonly includes silicification, sericitization, sulfidation and potassic alteration (e.g., Qiu et al., 2002). The dominant alteration paragenesis in the Linglong gold deposit is quartz, sericite, K-feldspar, albite, calcite and siderite. Ore minerals include pyrite as major phase and minor chalcopyrite, galena, sphalerite and hematite.

Numerous geochronological studies, involving direct and indirect dating of ore minerals, have been performed to constrain the mineralization age of the Linglong gold lode deposit hosted in the NNE-trending Linglong batholith. The batholith is composed of massive to strongly-foliated, medium- to coarse-grained biotite-bearing granites, which sporadically contain K-feldspar phenocrysts. Based on results from Rb–Sr and K–Ar methods on whole-rock and mineral, earlier studies reported mineralization ages varying from Early Proterozoic to Late Mesozoic (e.g., Li and Yang, 1993). K–Ar and Rb–Sr dating of hydrothermal alteration minerals, mineralized whole rocks or inclusions in quartz, gave more reasonable ages, ranging from 130 Ma to 80 Ma (e.g., Luo and Wu, 1987; Zhang et al., 1994). Wang et al. (1998) used the zircon U–Pb SHRIMP method to date the host rocks and feldspar porphyry dikes that cut the Linglong gold lode and placed a tight constraint on the gold mineralization age at about 125 Ma to 120 Ma. Yang and Zhou (2001) dated pyrite using the conventional Rb–Sr isochron method and suggested 123 Ma to 122 Ma as the time of gold mineralization.

3. Analytical methods

The Rb–Sr analyses in this study were performed in the Laboratory for Radiogenic Isotope Geochemistry (LRIG), Institute of Geology and Geophysics, Chinese Academy of

Table 1
Single grain minerals Rb–Sr analytical data of the Linglong gold mine

Sample		Rb (ppm)	Sr (ppm)	$^{87}Rb/^{86}Sr$	$^{87}Sr/^{86}Sr$ (2σ)
05LL-1 quartz	g1	0.024	0.061	1.15	0.71385±0.00014
	g2	0.027	0.144	0.54	0.71271±0.00014
	g3	0.056	0.098	1.64	0.71464±0.00010
	g4	0.686	0.313	6.36	0.72283±0.00008
	g5	1.077	0.516	6.03	0.72220±0.00002
05LL-8 sericite	g1	57.9	4.76	35.43	0.77143±0.00002
	g2	85.7	3.24	77.45	0.84453±0.00002
	g3	38.8	0.67	173.15	1.00514±0.00005
	g4	48.9	1.63	87.94	0.86373±0.00002
	g5	70.9	33.39	6.16	0.72241±0.00001
05LL-9 sericite	g1	37.5	0.36	324.8	1.27539±0.00013
	g2	36.6	1.20	91.0	0.86703±0.00002
	g3	22.6	0.53	126.2	0.92548±0.00005
	g4	15.9	0.24	196.0	1.04462±0.00010
	g5	23.2	0.23	303.7	1.23152±0.00012
05LL-1 pyrite	g1	0.106	0.080	3.87	0.71639±0.00007
	g2	0.054	0.056	2.80	0.71467±0.00029
	g3	0.041	0.126	0.95	0.71139±0.00007
	g4	0.047	0.080	1.71	0.71277±0.00014
05LL-2 pyrite	g1	1.22	0.20	18.11	0.73933±0.00007
	g2	0.45	0.13	9.67	0.72384±0.00004
	g3	0.79	0.08	28.59	0.75698±0.00008
	g4	0.42	0.09	14.16	0.73220±0.00006
	g5	1.00	0.15	19.40	0.74076±0.00007
	g6	0.36	0.08	12.81	0.73025±0.00007
	g7	0.99	0.42	6.81	0.71990±0.00004
	g8	0.58	0.17	10.12	0.72560±0.00014
	g9	1.16	0.12	27.21	0.75447±0.00014
05LL-3 pyrite	f1	2.13	3.45	1.79	0.71467±0.00004
	f2	0.61	1.52	1.16	0.71365±0.00007
	f3	1.23	1.41	2.53	0.71602±0.00006
	f4	2.21	3.50	1.82	0.71470±0.00007
	f5	0.95	1.75	1.57	0.71434±0.00006
05LL-9 pyrite	f1	2.72	0.51	15.55	0.73754±0.00007
	f2	0.76	0.19	11.63	0.73050±0.00029
	f3	1.28	0.39	9.52	0.72655±0.00015
	f4	2.19	0.46	13.92	0.73428±0.00011
	f5	0.46	0.21	6.39	0.72114±0.00022
	f6	0.21	0.22	2.76	0.71518±0.00014

Sample weight for analysis: about 0.1 mg of sericite, 3–5 mg of quartz, and 1–3 mg of pyrite for each fraction. g: whole grain; f: fragment.

Sciences (IGG CAS). Reagents were doubly distilled in a FEP-Teflon 2-bottle still. A Millipore-Element apparatus produces 18.2 MΩ purified water containing <0.2 pg/ml of Sr and Rb.

Minerals were separated from small specimens (about 2×2×3 cm in size) to minimize the problem of isotopic disequilibrium and hand-picked under a binocular microscope. Mineral grains were transferred into Teflon® vessels, after being washed ultrasonically in analysis-grade alcohol and Millipore water. Pyrite grains were dissolved using 0.3 ml 3N HNO_3 and 0.1 ml HF at 80 °C. For sericite and quartz, the vapor digestion method was applied for sample digestion (Li et al., 2005). A rack with sample vessels placed in sequence was put in a Teflon® bomb filled with 2 ml HF and 0.2 ml HNO_3 at the bottom. The bomb was then put in a steel cell to hold required pressure. The samples were dissolved at about 190 °C for 48 h. HF acid solution remaining in the vessels was dried and replaced by 0.1 ml 3N HNO_3. Then the vessels were heated to dry again to convert fluoride salts into more soluble nitrate salts. 0.2 ml 3N HNO_3 was added to the vessels after being cooled down to room temperature. A mixed ^{87}Rb–^{84}Sr spike solution was used as spike.

Separation and purification of Rb and Sr were done on Teflon® mini-columns filled with about 0.1 ml Sr-spec® resin following the procedure of Horwitz et al. (1992). Pure Sr samples were loaded on single tungsten filaments and a purified Ta–HF solution was used as emitter. Isotopic ratios of Rb and Sr were measured on an IsoProbe-T mass spectrometer at LRIG. Correction of mass fractionation for Sr isotopic ratios was based on an $^{88}Sr/^{86}Sr$ value of 8.37521 using a power law. During this study, repeated measurements on NBS 987 Sr standard solution gave $^{87}Sr/^{86}Sr$ mean values of 0.710242±16 (2σ, n=12, with

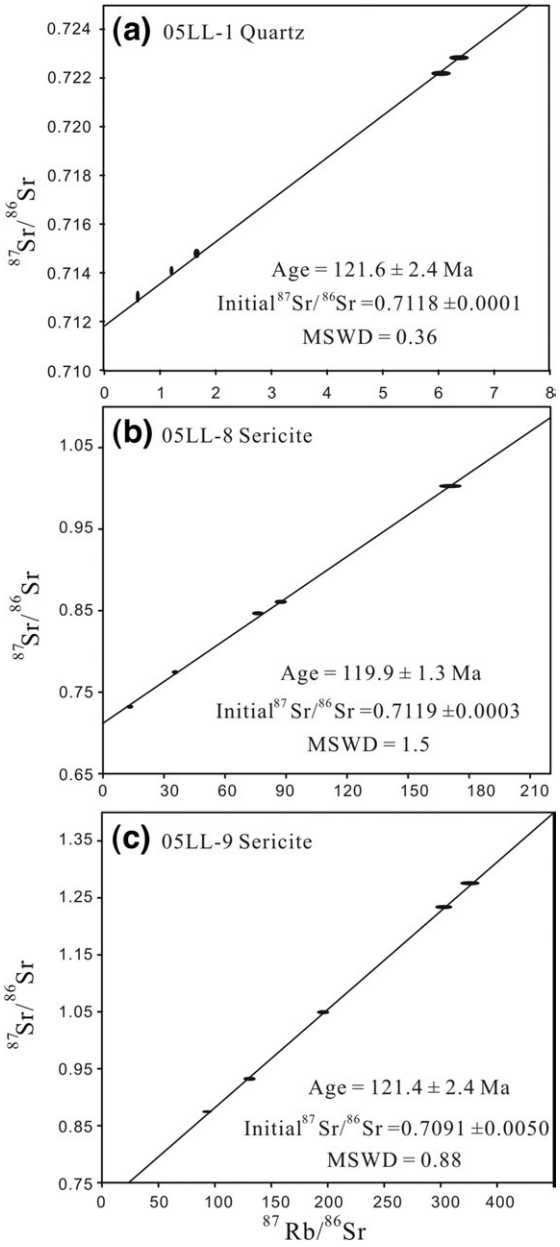

Fig. 2. Rb–Sr analytical data of single grain quartz (a) and sericite (b, c) samples.

loads of 100 ng Sr per run) and 0.710250±31 (2σ, n=6, 200 pg Sr per run). During the course of this study, procedural blanks for Rb and Sr were 4±1 pg and 6±1 pg (n=6), respectively. More detailed descriptions of the analytical procedures are provided in Li et al. (2005).

Mineral inclusions in pyrite were identified with an LEO 1450VP scanning electron microscope (SEM) equipped with an INCA ENERGY 300 X-ray Energy Dispersive Spectrometer (EDS) system. Pyrite grains were mounted in epoxy and then polished down to half sections. The SEM produces high resolution images to show well-marked inclusions, which were assessed semi-quantitatively by EDS analyses.

4. Analytical results

Pyrite, sericite, and quartz investigated in this study were separated from five samples of ore veins collected from the Linglong gold mine (Fig. 1). Rb–Sr analytical data of single grain minerals are given in Table 1. Data regression for isochron ages and weighted mean values were done with the ISOPLOT software (Ludwig, 2001), using 2% error for $^{87}Rb/^{86}Sr$ ratios and the within-run measurement precision for $^{87}Sr/^{86}Sr$ values (2σ).

Sample 05LL-1 was collected from a white quartz vein presenting an earlier mineralization stage (Chen et al., 1989). Less sulfide minerals, mainly cubic pyrite, scatter in the vein. SEM studies show that pyrite from this sample contains rare and tiny mineral inclusions including sericite and ilmenite (Fig. 4). An Rb–Sr isochron defined by five quartz grains yields an age of 121.6±2.4 Ma (Fig. 2a), consistent with the Rb–Sr age (121.1±3.9 Ma, Fig. 3a) defined by four pyrite grains from the same sample.

Sample 05LL-2 is a smoky gray quartz vein from the main mineralization stage according to Chen et al. (1989). Sulfide minerals in the vein include pyrite, minor chalcopyrite, galena and sphalerite. Pyrite occurs as pentagonal dodecahedron. SEM studies show that pyrite contains the following mineral inclusions: frequent sericite, minor K-feldspar, zircon and quartz. An Rb–Sr isochron defined by nine pyrite grains yields an age of 120.2±3.7 Ma (Fig. 3b) with $^{87}Rb/^{86}Sr$ ratios ranging from 6.8 to 28.6.

Sample 05LL-3 was collected from a K-feldspar alteration and sericitization zone with fine pyrite veins. SEM studies indicate that pyrite contains mainly albite and minor sericite. Five pyrite grains give an Rb–Sr isochron age of 120±6.7 Ma (Fig. 3c).

Sample 05LL-8 was collected from a pre-existing fracture filled with thin zones of quartz and sericite. No sulfide minerals are found in these zones. The sericite separated from this sample yielded an Rb–Sr isochron age of 119.9±1.3 Ma (Fig. 2b).

Sample 05LL-9 was collected from a pyrite–sericite alteration zone. SEM studies show that pyrite mainly contains sericite and minor albite and quartz. Sericite gave an Rb–Sr isochron age of 121.4±2.4 Ma (Fig. 2c), consistent with the pyrite Rb–Sr isochron age of 121±2 Ma.

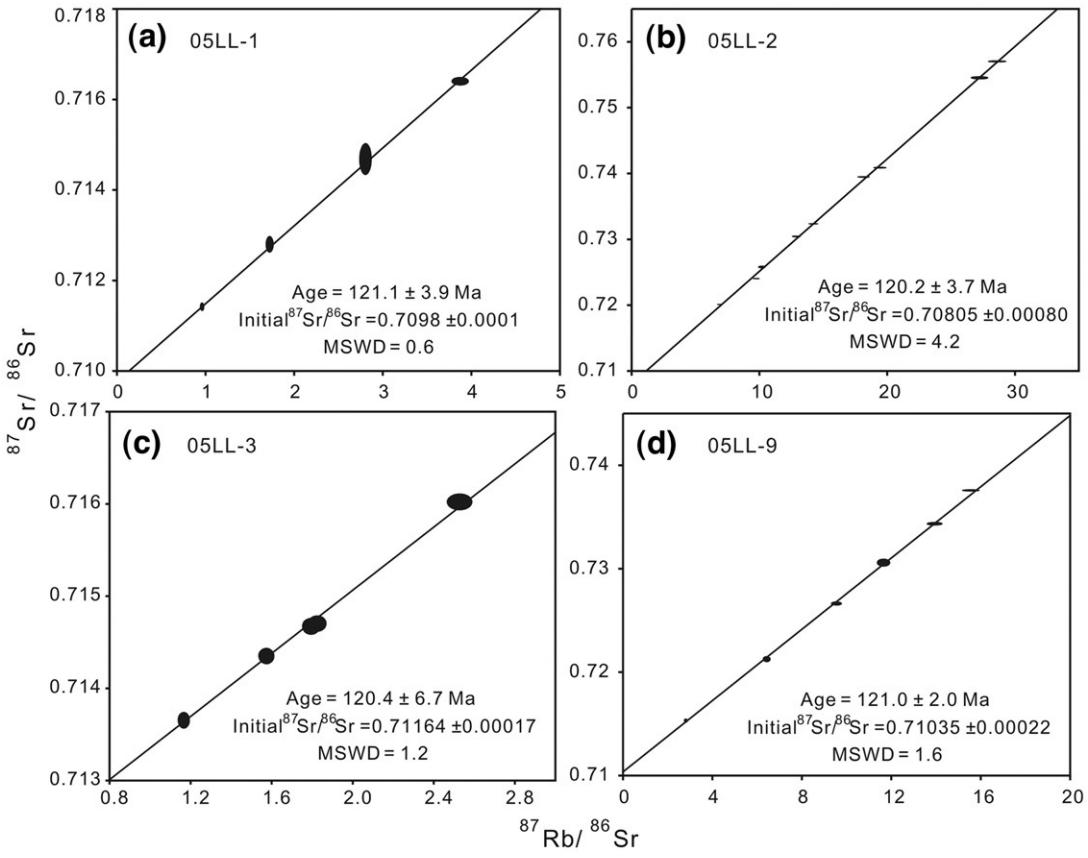

Fig. 3. Rb–Sr analytical data of single grain pyrite samples.

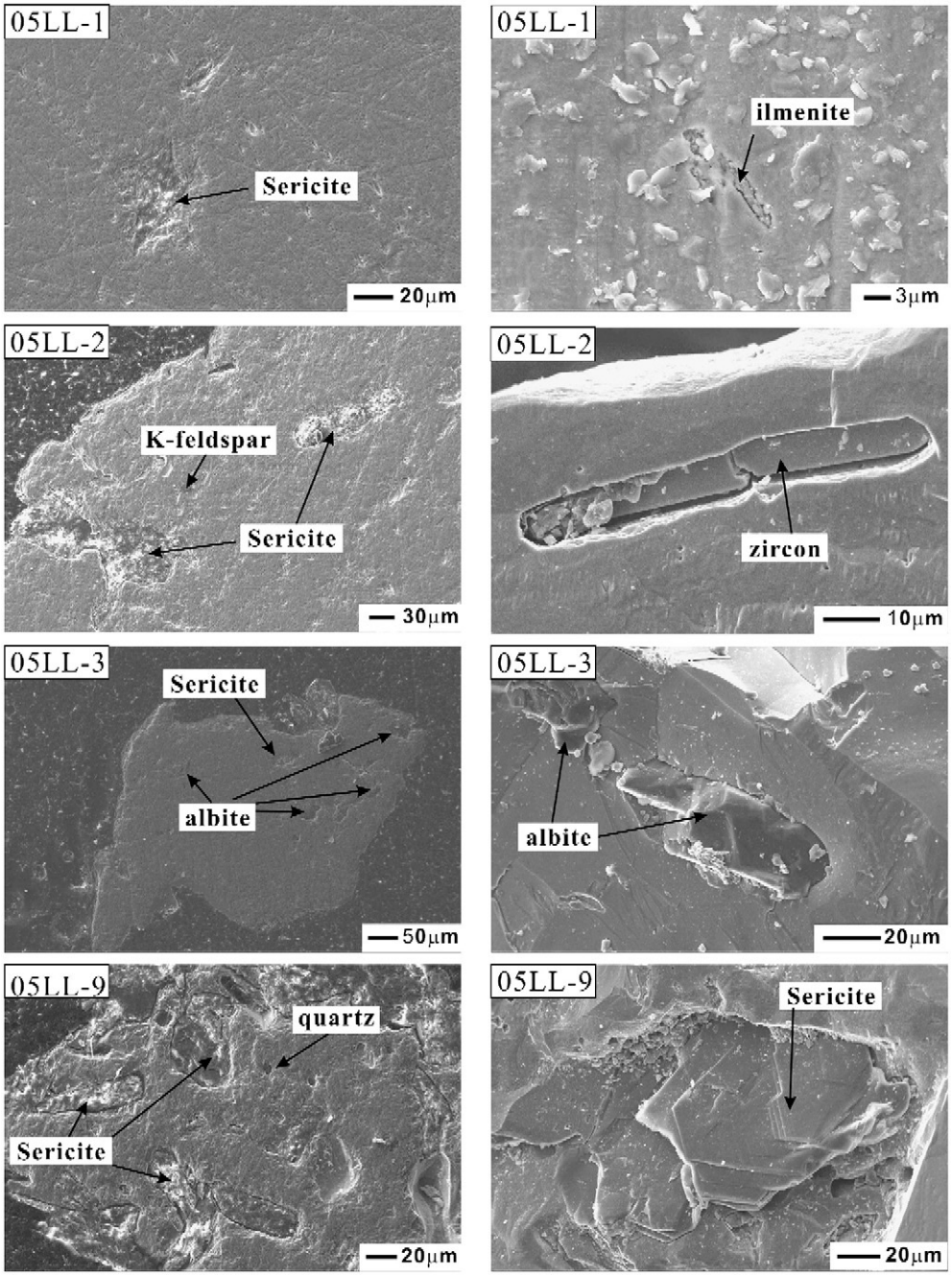

Fig. 4. Mineral inclusions in pyrite imaged by the scanning electron microscope. Sericite inclusion can be found in most pyrite grains from all four samples. Pyrite grains of samples 05LL-2, 05LL-3 and 05LL-9 also contain albite, K-feldspar, and quartz inclusion; sample 05LL-3 contains albite inclusions. Ilmenite and zircon were found as inclusion in samples 05LL-2 and 05LL-1, respectively.

The analyzed grains contain variable Rb and Sr concentrations, resulting in variable $^{87}Rb/^{86}Sr$ ratios (Table 1). A weighted mean value of 120.6±0.9 Ma (MSWD=0.42) can be calculated from all seven isochron ages. The isochron ages obtained by the single grain technique are consistent, within errors, with ages of 123 Ma to 122 Ma obtained by conventional Rb–Sr dating using the leaching technique (Yang and Zhou, 2001). Initial $^{87}Sr/^{86}Sr$ ratios obtained from the interceptions of the isochrons range from 0.7080 to 0.7119, indicating that different fluids were involved in mineral precipitation. From Sr–Nd–Pb isotopic evidence of pyrite, Yang and Zhou (2001) have already shown that fluids responsible for the ore mineralization were derived from a mixture of fluids originating from degassing of mafic magmas and meteoric water that had leached the wall rocks of the Linglong gold mine.

5. Discussion

The analyzed pyrite grains from four different samples of the Linglong gold deposit contain variable Rb and Sr concentrations

and show large variations in Rb/Sr ratios. SEM investigations show that pyrite from different samples contains distinct mineral inclusions including sericite, albite, quartz and K-feldspar ranging from of one to tens of μm in size (Fig. 4). Rutile, zircon and ilmenite are also found occasionally as inclusions in pyrite. Fluid inclusions and micro-inclusions of minerals have been identified by SEM examination of different pyrite types from the Proterozoic Black Reef in South Africa (Barton and Hallbauer, 1996). A correlation between mineral inclusions, Rb and Sr content and Rb/Sr ratios would be therefore likely to exist. Pyrites from samples 05LL-2 and 05LL-9 have distinctly higher $^{87}Rb/^{86}Sr$ ratios due to contribution of Rb from mineral inclusions mainly of sericite. In contrast, pyrite from sample 05LL-3, collected from a feldspatized vein, contain mainly tiny albite inclusions and hence have high Sr contents, resulting in low $^{87}Rb/^{86}Sr$ ratios between 1.2 and 2.5. Rare, but small sericite was found as inclusions in pyrite from the quartz vein (05LL-1). These grains have lower Rb and Sr concentrations; the $^{87}Rb/^{86}Sr$ ratios range from 0.95 to 3.9. Previous studies have shown that Rb and Sr hosted in pyrite may occur in fluid inclusions (Lüders and Ziemann, 1999; Yang and Zhou, 2001). Nevertheless, the results of this study indicate that the variation of Rb/Sr, Rb and Sr concentrations is largely controlled by mineral inclusions in pyrite and hence, the dating results can be significantly influenced, especially by mica and feldspar. If isotopic equilibrium between the mineral inclusions and the pyrite host was attained during hydrothermal activity, or host and inclusion-forming minerals crystallized simultaneously, the dating results can indeed represent the crystallization time of pyrite and thus, the mineralization time of the ore deposit. Although different mineral inclusions occur in pyrite samples collected from different veins, isochrons obtained by the single grain pyrite Rb–Sr analysis give consistent age values between 122 Ma and 120 Ma. These age data are also consistent with ages obtained from quartz and sericite separated from the same hand specimen. The correspondence between the Rb–Sr ages of different minerals suggests simultaneous crystallization or isotopic equilibrium between mineral (and/or fluid) inclusions and their host pyrite during the gold mineralization.

Owning to limitation of high procedural blank and insufficient sensitivity of TIMS technique, large amounts of sample material were traditionally usually used for conventional Rb–Sr isochron analyses of different minerals and/or whole rocks. The results often show wide range or large errors (e.g. Zhang et al., 1994), indicating isotopic disequilibrium among different specimens or minerals. In this study, the Rb–Sr isochrons defined by single grain minerals from small specimens suggest that a given mineral can achieve isotopic equilibrium, thus providing meaningful ages. This single grain Rb–Sr analytical technique requires a combination of low (pg level) procedural Rb and Sr blank values and sensitive mass spectrometers enabling high-precision measurement of single grain minerals or micro samples. Pyrite, quartz and sericite often occur in ore deposits and are genetically related to the mineralization. Therefore, the single grain Rb–Sr dating technique can significantly promote applications of direct dating of hydrothermal mineral deposits in future. It can also meet the need for the Rb–Sr isotopic analysis on complicated metamorphic rocks and samples with low Rb and Sr concentrations.

In summary, pyrites from the Linglong gold deposit have variable Rb and Sr contents, causing variation in Rb/Sr ratios that facilitates single grain Rb–Sr isochron dating. Rb and Sr in pyrite may not only occur in fluid inclusions, as suggested in previous studies, but also originate from mineral inclusions such as sericite and feldspar. If isotopic equilibrium between mineral inclusions and host pyrite was attained during hydrothermal activity, geologically meaningful ages can be obtained for the formation time of an ore deposit by the single grain Rb–Sr technique.

Acknowledgments

This study was financially supported by the Ministry of Science and Technology of China (Project No. 2006CB403505) and by the Natural Science Foundation of China (Project Nos. 40525007 and 40403008). Sincere thanks are due to Drs. R. Ayuso and B. Bruce for constructive comments and suggestions for improvement of the manuscript, Dr. W. Siebel for improvement in English and discussion, X.-H. Li and P. Xiao for their help in the Rb–Sr analysis and X. Yan for guidance in operation of the scanning electron microscope.

References

Barra, F., Ruiz, J., Mathur, R., Titley, S., 2003. A Re–Os study of sulfide minerals from the Bagdad porphyry Cu–Mo deposit, northern Arizona, USA. Mineralium Deposita 38, 585–596.

Barton, E.S., Hallbauer, D.K., 1996. Trace-element and U–Pb isotope compositions of pyrite types in the Proterozoic Black Reef, Transvaal Sequence, South Africa: implications on genesis and age. Chemical Geology 133, 173–199.

Brannon, J.C., Pldosek, F.A., Mclimans, R.K., 1992. Alleghenian age of the Upper Mississippi Valley zinc–lead deposit determined by Rb–Sr dating of sphalerite. Nature 356, 509–511.

Böhlke, J.K., Kistler, R.W., 1986. Rb–Sr, K–Ar, and stable isotope evidence for the ages and sources of fluid components of gold-bearing quartz veins in the northern Sierra Nevada Foothills metamorphic belt, California. Economic Geology 81, 296–322.

Charlier, B.L.A., Ginibre, C., Morgan, D., Nowell, G.M., Pearson, D.G., Davidson, J.P., Ottley, C.J., 2006. Methods for the microsampling and high-precision analysis of strontium and rubidium isotopes at single crystal scale for petrological and geochronological applications. Chemical Geology 232, 114–133.

Chen, C.-H., DePaolo, D.J., Lan, C.-Y., 1996. Rb–Sr microchrons in the Manaslu granite: Implications for Himalayan thermochronology. Earth and Planetary Science Letters 143, 125–135.

Chen, G.Y., Shao, W., Sun, D.S., 1989. Genetic Mineralogy of Gold Deposits in Jiaodong Region with Emphasis on Gold Prospecting. Chongqing Publishing House, Chongqing, pp. 181–224 (in Chinese with English abstract).

Chen, Y.-J., Pirajno, F., Lai, Y., Li, C., 2005. Origin of gold metallogeny and sources of ore-forming fluids, Jiaodong Province, eastern China. International Geology Review 47, 530–549.

Fan, H.-R., Zhai, M.-G., Xie, Y.-H., Yang, J.-H., 2003. Ore-forming fluids associated with granite-hosted gold mineralization at the Sanshandao deposit, Jiaodong gold province, China. Mineralium Deposita 38, 739–750.

Fan, H.-R., Hu, F.-F., Yang, J.-H., Shen, K., Zhai, M.-G., 2005. Fluid evolution and large-scale gold metallogeny during Mesozoic tectonic transition in the eastern Shandong province. Acta Petrologica Sinica 21, 1317–1328.

Frei, R., Nägler, T., Schönberg, R., Kramers, J., 1998. Re–Os, Sm–Nd, U–Pb and stepwise lead leaching isotope systematics in shear zone hosted gold

mineralization: genetic tracing and age constraints of crustal hydrothermal activity. Geochimica et Cosmochimica Acta 62, 1925–1936.

Frei, R., Bridgwater, D., Rosing, M., Stecher, O., 1999. Controversial Pb–Pb and Sm–Nd isotope results in the early Archean Isua (West Greenland) oxide iron formation: preservation of primary signatures versus secondary disturbances. Geochimica et Cosmochimica Acta 63, 473–488.

Freydier, C., Ruiz, J., Chesley, J., McCandless, T., Munizaga, F., 1997. Re–Os isotope systematics of sulfides from felsic igneous rocks: application to base metal porphyry mineralization in Chile. Geology 25, 775–778.

Guan, K., Luo, Z.-K., Miao, L.-C., Huang, J.-Z., 1998. SHRIMP in zircon chronology for Guojialing suite granite in Jiaodong district. Scientia Geologica Sinica 33, 318–328 (in Chinese with English abstract).

Horwitz, E.P., Chiarizia, R., Dietz, M.L., 1992. A novel strontium-selective extraction chromatographic resin. Solvent Extraction and Ion Exchange 10, 313–336.

Ji, H., Shimazaki, H., Hu, S., Zhao, Y., 1994. Two types of greenstone belts in the Shandong Province, eastern China. Resource Geology 44, 101–110.

Jiang, S.-Y., Slack, J.-F., Palmer, M.R., 2000. Sm–Nd dating of the giant Sullivan Pb–Zn–Ag deposit, British Columbia. Geology 28, 751–754.

Lambert, D.D., Foster, J.G., Frick, L.R., 1999. Re–Os isotope geochemistry of magmatic sulfide ore systems. Reviews in Economic Geology 12, 29–57.

Li, J.-W., Vasconcelos, P.M., Zhang, J., Zhou, M.-F., Zhang, X.-J., Yang, F.-H., 2003. $^{40}Ar/^{39}Ar$ constraints on a temporal link between gold mineralization, magmatism, and continental margin transtension in the Jiaodong gold province, eastern China. Journal of Geology 111, 741–751.

Li, Q.-L., Chen, F., Wang, X.-L., Li, X.-H., Li, C.-F., 2005. Ultra-low procedural blank and the single-grain mica Rb–Sr isochron dating. Chinese Science Bulletin 50, 2861–2865.

Li, Z.-L., Yang, M.-Z., 1993. The Geology and Geochemistry of Gold Deposits in the Jiaodong Region. Tianjin Science and Technology Press. 300 pp. (in Chinese).

Lüders, V., Ziemann, M., 1999. Possibilities and limits of infrared light microthermometry applied to studies of pyrite-hosted fluid inclusions. Chemical Geology 154, 169–178.

Ludwig, K.R., 2001. Users Manual for Isoplot/Ex: A Geochronological Toolkit for Microsoft Excel. Berkeley Geochronology Center Special Publication, USA, pp. 1–53.

Luo, W.-C., Wu, Q.-S., 1987. Dating of the mineralizing age of gold deposits in Jiaodong Peninsula using the alteration minerals. Chinese Science Bulletin 16, 1245–1248.

McCandless, R.E., Ruiz, J., Campbell, A.R., 1993. Rhenium behavior in molybdenite in hypogene and near-surface environments: implications for Re–Os geochronometry. Geochimica et Cosmochimia Acta 57, 889–905.

Miao, L.-C., Lou, Z.-K., Huang, J.-Z., Guan, K., Wang, L.-G., McNaughton, N.J., Groves, D.I., 1997. Zircon Sensitive High Resolution Ion Microprobe (SHRIMP) study of granitoid intrusions in Zhaoye gold belt of Shandong Province and its implication. Science in China (Series D) 40, 361–369.

Morelli, R.M., Creaser, R.A., Selby, D., Kelley, K.D., Leach, D.L., King, A.R., 2004. Re–Os sulfide geochronology of the Red Dog sediment-hosted Zn–Pb–Ag deposit, Brooks Range, Alaska. Economic Geology 99, 1569–1576.

Müller, W., Aerden, D., Halliday, A.N., 2000a. Isotopic dating of strain fringe increments: duration and rates of deformation in shear zones. Science 288, 2195–2198.

Müller, W., Mancktelow, N.S., Meier, M., 2000b. Rb–Sr microchrons of synkinematic mica in mylonites: an example from the DAV fault of the Eastern Alps. Earth and Planetary Science Letters 180, 385–397.

Nakai, S., Halliday, A.N., Kesler, S.E., Jones, H.D., 1990. Rb–Sr dating of sphalerites from Tennessee and the genesis of Mississippi Valley type ore deposits. Nature 346, 354–357.

Philips, D., Miller, J.M., 2006. 40Ar/39Ar dating of mica-bearing pyrite from thermally overprinted Archean gold deposits. Geology 34, 397–400.

Qiu, Y.-S., 1989. Regional Geological Setting of Gold Deposits in the Zhaoye Gold Belt in Shandong Province. Liaoning Science and Technology Press, Shenyang, China. 153 pp. (in Chinese).

Qiu, Y.-M., Groves, D.I., McNaughton, N.J., Wang, L.-G., Zhou, T.-H., 2002. Nature, age, and tectonic setting of granitoid-hosted, orogenic gold deposits of the Jiaodong Peninsula, eastern North China craton, China. Mineralium Deposita 37, 283–305.

Smith, P.E., Evensen, N.M., York, D., Szatmari, P., de Oliveria, D.C., 2001. Single-crystal $^{40}Ar–^{39}Ar$ dating of pyrite: no fool's clock. Geology 29, 403–406.

Stein, H.J., Morgan, J.W., Schersten, A., 2000. Re–Os dating of low-level highly radiogenic (LLHR) sulfides: the Harnäs gold deposit, Southwest Sweden, records continental-scale tectonic events. Economic Geology 95, 1657–1671.

Trista-Aguilera, D., Barra, F., Ruiz, J., Morata, D., Talaera-Mendoza, O., Kojima, S., Feraris, F., 2006. Re–Os isotope systematics for the Lince-Estefania deposit: constraints on the timing and source of copper mineralization in a stratabound copper deposit, Coastal Cordillera of Northern Chile. Mineralium Deposita 41, 99–105.

Villa, I.M., 1998. Isotopic closure. Terra Nova 10, 42–47.

Wang, L.-G., Qiu, Y.-M., McNaughton, N.J., Groves, D.L., Luo, Z.-K., Huang, J.-Z., Miao, L.-C., Liu, Y.-K., 1998. Constraints on crustal evolution and gold metallogeny in the northeastern Jiaodong Peninsula, China, from SHRIMP U–Pb zircon studies of granitoids. Ore Geology Reviews 13, 275–291.

Yang, J.-H., Zhou, X.-H., 2001. Rb–Sr, Sm–Nd and Pb isotope systematics of pyrite: Implications for the age and genesis of lode gold deposits. Geology 29, 711–714.

Yang, J.-H., Wu, F.-Y., Wilde, S.A., 2003. A review of the geodynamic setting of large-scale Late Mesozoic gold mineralization in the North China craton: an association with lithospheric thinning. Ore Geology Reviews 23, 125–152.

Zhai, M.-G., Cong, B.-L., Guo, J.-H., Wang, Q.-C., 2000. Sm–Nd geochronology and petrography of garnet pyroxene granulites in the northern Sulu region of China and their geotectonic implication. Lithos 52, 23–33.

Zhai, M.-G., Yang, J.-H., Fan, H.-R., Miao, L.-C., Li, Y.-G., 2002. A large-scale cluster of gold deposits and metallogenesis in the Eastern North China craton. International Geology Review 44, 458–476.

Zhang, L.-C., Shen, Y.-C., Liu, T.-B., Zeng, Q.-D., Li, G.-M., Li, H.-M., 2003. $^{40}Ar/^{39}Ar$ and Rb–Sr isochron dating of the gold deposits on northern margin of the Jiaolai Basin, Shandong, China. Science in China (D) 46, 708–718.

Zhang, Z.-H., Zhang, J.-X., Ye, S.-Z., 1994. Isotopic Age of Gold Deposits in Jiaodong Peninsula. Seismology Press, Beijing, China, pp. 1–56 (in Chinese).

Zheng, Y.-F., 1989. Influence of the nature of the initial Rb–Sr system on isochron validity. Chemical Geology 80, 1–16.